Electronic Supplementary Information

Structure and single-molecule conductance of two endohedral metallofullerenes with large C_{88} cage

Wang Li[1], Fayu Qu[2], Linshan Liu[1,3], Zhuxia Zhang[3], Chaofeng Zheng[1], Lin Wang*[2], Chunru Wang[1], and Taishan Wang*[1]

[1]*Beijing National Laboratory for Molecular Sciences, Key Laboratory of Molecular Nanostructure and Nanotechnology, Institute of Chemistry, Chinese Academy of Sciences, Beijing 100190, China*
[2]*School of Materials Science and Technology, China University of Geosciences, Beijing 100083, China*
[3]*College of Chemistry, Taiyuan University of Technology, Taiyuan 030024, China*

1. Experimental details

(1) Synthesis and HPLC separation of $Ce_2O@C_{88}$ and $Ce_3N@C_{88}$.

The detailed experimental procedures were produced by arc-discharge method. Briefly, core-drilled graphite rods (Φ 8 mm × 120 mm) filled with CeO_2 and graphite powder (Ce: C mass ratio 3: 2) were evaporated in an arc generator under helium atmosphere (250 Torr) to get the raw carbon soot. Soxhlet extraction was then performed using toluene as solvent at 260 ℃ for 12 h. After getting the concentrated solution rich of metallofullerenes, multiple-stage HPLC separation was performed on Buckyprep and Buckyprep-M column (20 mm × 250 mm) in succession with toluene as mobile phase. After collecting the corresponding eluent fraction that was rich in $Ce_2O@C_{88}$ and $Ce_3N@C_{88}$, pure samples of $Ce_2O@C_{88}$ and $Ce_3N@C_{88}$ were finally obtained after HPLC cycling separation.

(2) UV-vis-NIR absorption spectra and Raman spectra of $Ce_2O@C_{88}$ and $Ce_3N@C_{88}$.

UV-vis-NIR absorption spectra were measured in toluene on a Hitachi UH-4150 spectrophotometer. Raman spectra were measured on a Renishaw/inVia-Qontor apparatus with a laser source of 532 nm.

(3) DFT calculations of $Ce_2O@C_{88}$ and $Ce_3N@C_{88}$.

Geometry optimization were performed without symmetry constraints using the Gaussian 09 optimizer at the level of B3LYP/6-31G* with the inclusion of considering the dispersion corrections on the corresponding complex structures (SDD for Ce,6-31G* for C)

(4) STM-BJ measurements of $Ce_2O@C_{88}$ and $Ce_3N@C_{88}$.

Single-molecule conductance measurements were carried out using Xtech STM-BJ developed by Prof. Wenjing Hong's group[S1], and the data is analyzed by XMe opensource code (https://github.com/Pilab-XMU/XMe_DataAnalysis). The Au substrate was prepared by evaporating ~100 nm Au onto silicon wafer (purchased from Beijing Topvendor Technology Co., Ltd.) and then cleaned by piranha solution (7:3 concentrated H_2SO_4/H_2O_2) before each experiment. The gold tip was made by flame cleaning of gold wires (0.25 nm diameter, Pram corporation, 99.99%) to form a gold bead. Conductance of the fullerene derivatives were measured in a Teflon cell filled with 0.003 mM ($Ce_3N@C_{88}$) and 0.003 mM ($Ce_2O@C_{88}$) molecular solution (volume ratio of the mixed solvent, VMB: VTMB = 1:4) in the ambient atmosphere. The cell was preliminarily dipped in piranha solution and then washed by sonication in Milli-Q water (18.2 MΩ, TOC ⩽4 ppb) for several times.

For each molecule, we repeatedly formed and broke Au point contacts with the tip approaching to/retracting from the substrate at a speed of 18 nm/s and recorded the traces of conductance versus displacement as the tip was withdrawn. We collected more than 1000 traces for every measurement at different positions of the substate. Data in each experiment was acquired and analyzed with a lab-made program in LabView 2016. All the traces were recorded consecutively and automatically. At least two independent experiments were conducted to ensure that the results are reproducible.

In one-dimensional (1D) histogram, we can observe several sharp statistical peaks corresponding to G_0, $2G_0$, $3G_0$ …, indicating that the gold electrodes break step by step and the atomic interface has been formed facilitating the single-molecule measurement. The most probable conductance peak was fitted by Gauss distribution. Then, we compiled all the conductance-displacement traces to construct the two-dimensional (2D) histogram, from which the geometric information of the molecular junction can be deduced. We introduced a relative distance (Δz) and defined Δz = 0 at $10^{-0.3}$ G_0 to align all the stretching curves. Bright features, showing gold–gold contacts, can be seen around $G = G_0$, followed by another well-defined conductance scatter group in the range of $10^{-1.0}$ G_0 ~$10^{-2.0}$ G_0.

To construct the stretching distance distribution histograms, firstly the relative stretching distance, z, is determined from the position where the conductance is $10^{-0.3}$ G_0 (after the rupture of the gold-gold atomic point contact at G_0), to the molecular conductance region, just before the end of molecular plateau. The peak represents the most probable stretching length of the single-molecule junction. The corrected elongation of the molecular junction should be the sum of the most probable stretching length and the snap-back distance of the gold electrodes determined experimentally to be 0.6-0.8 nm.

In the mixed solvent, there is no conductance peak in the 1D and 2D histogram (Figure S1). For $Ce_2O@C_{88}$, the 2D histogram composed by all data show that a certain number of curves have no conductance plateau (Figure S2). In addition, we observed some of the curves demonstrating a plateau around $10^{-1.0}$ G_0. We propose a selecting criterion that the stretching length should be longer than 0.2 nm at $10^{-2.0}$ G_0 and construct the 1D histogram in Figure 5c.

2. Additional data from STM-BJ measurements.

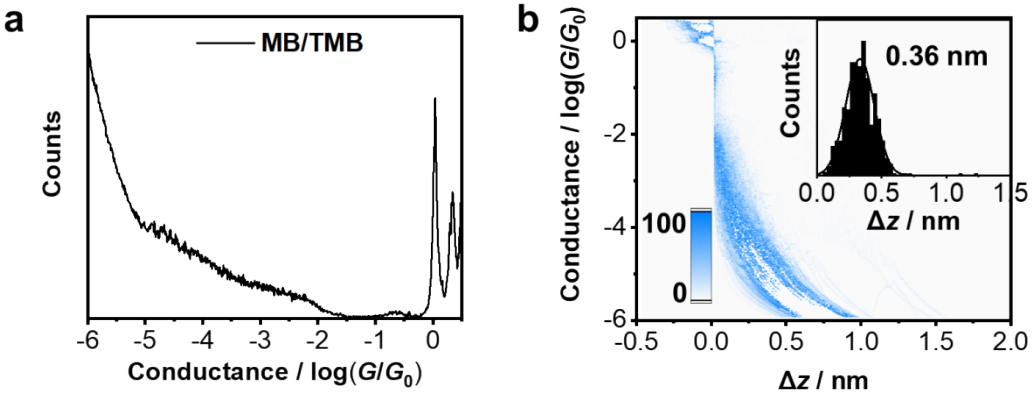

Figure S1. Clean background in the conductance histogram of the mixed solvent (V_{MB}: V_{TMB}= 1: 4). (a) 1D histogram. (b) 2D histogram and stretching distance Δz distributions (inset) of solvent (from $10^{-0.3}$ G_0 to $10^{-5.0}$ G_0).

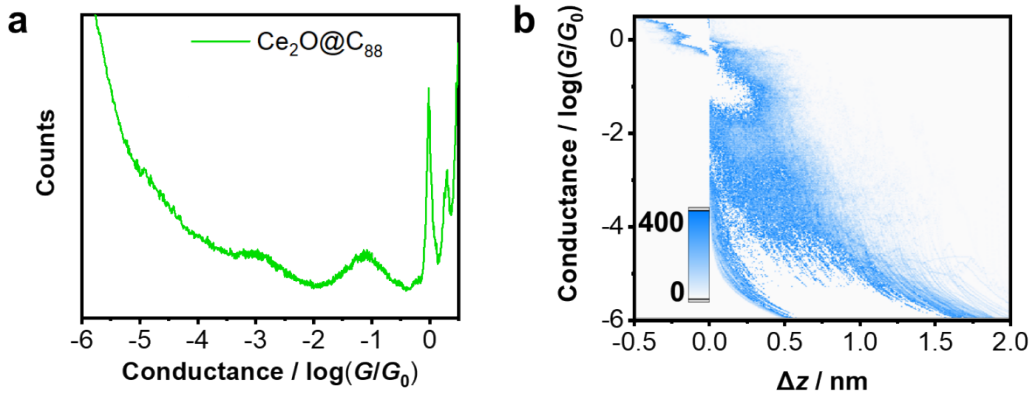

Figure S2. 1D and 2D conductance histograms of $Ce_2O@C_{88}$ based on the non-selected conductance-distance curves.

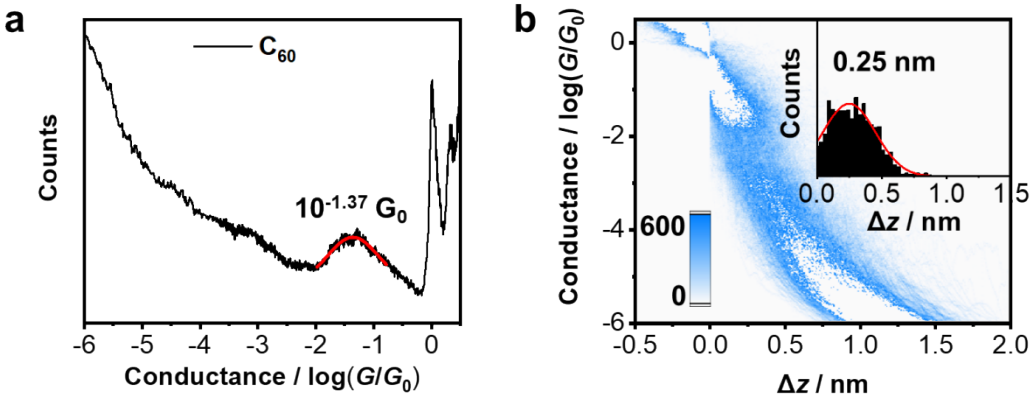

Figure S3. Conductance measurement results of C_{60}. (a) 1D histogram. (b) 2D histogram and stretching distance Δz distributions (inset) of C_{60} (from $10^{-0.3}$ G_0 to $10^{-2.0}$ G_0).

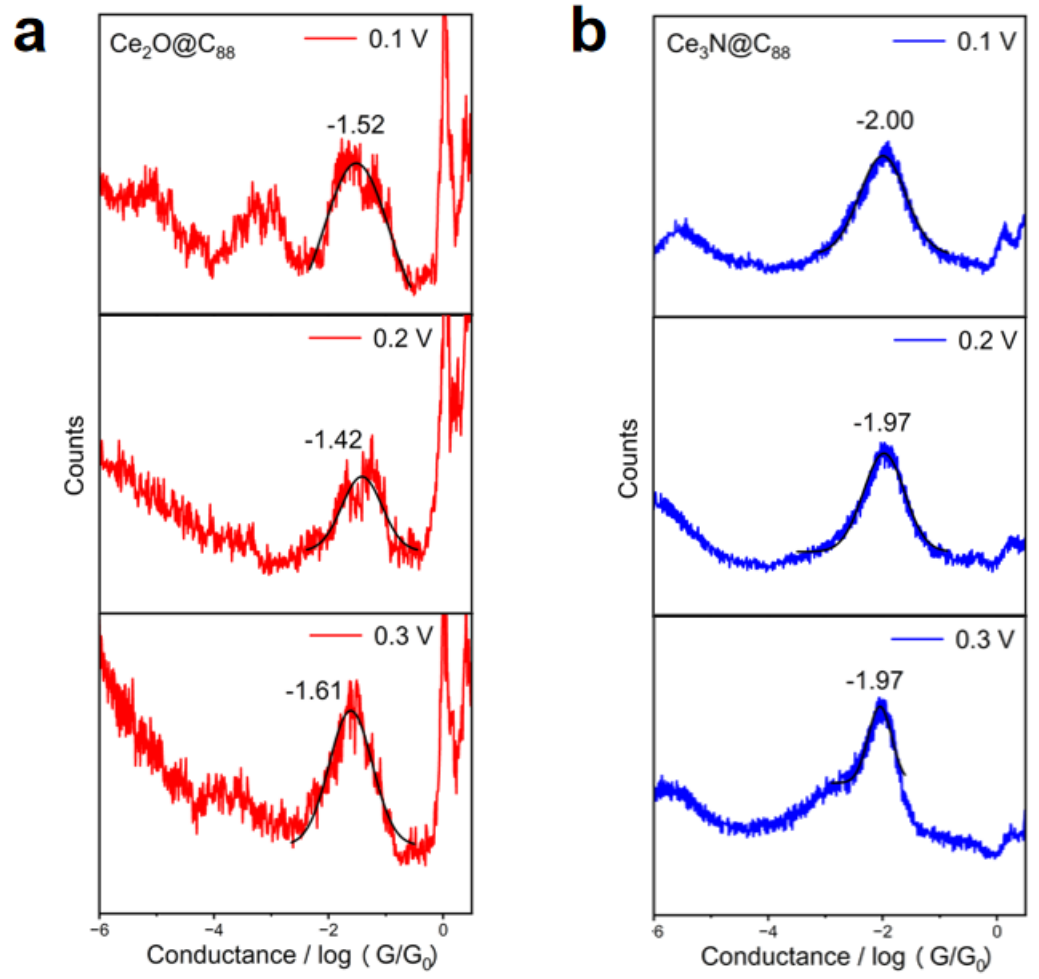

Figure S4. Conductance histograms of (a) $Ce_2O@C_{88}$ and (b) $Ce_3N@C_{88}$ based on the selected conductance-displacement curves at different bias from 0.1 V to 0.3 V.

3. **The coordinates for optimized compounds at the theory level of B3LYP-D3/6-31G*~ECP(ECP=MWB28 for Ce)**

(1) The coordinates of optimized $Ce_2O@D_2(35)$-C_{88}

C	-0.63396800	-4.42998800	0.37268600
C	0.63442300	-4.42994500	-0.37247100
C	-1.85041700	-4.15554500	-0.32909000
C	1.85083200	-4.15531600	0.32928400
C	-0.61089400	-4.06725900	1.75399100
C	0.61132300	-4.06730600	-1.75381100
C	-1.81941300	-3.74612800	-1.71584600
C	1.81975800	-3.74581100	1.71600500
C	-0.61666800	-3.65792600	-2.39013800
C	0.61702900	-3.65770700	2.39026900
C	-2.94211500	-3.46178100	0.27754600
C	2.94246100	-3.46150300	-0.27737500
C	-1.66359700	-3.29680000	2.33587800
C	1.66397700	-3.29676200	-2.33574400
C	-2.84228200	-2.98856300	1.61661000
C	2.84262600	-2.98836200	-1.61645400
C	-2.83746900	-2.76902700	-1.95155600
C	2.83765200	-2.76858100	1.95165400
C	-0.34823300	-2.53430600	-3.25044800
C	0.34846400	-2.53409900	3.25052300
C	-3.60866000	-2.63707500	-0.72593900
C	3.60885200	-2.63662100	0.72608200
C	-1.05974300	-2.32202100	3.24227100

C	1.05999200	-2.32205200	-3.24218900
C	-2.58510300	-1.64366100	-2.78374300
C	2.58514500	-1.64323400	2.78379800
C	-3.50961300	-1.76364700	1.94096000
C	3.50985500	-1.76334500	-1.94081900
C	-1.26246100	-1.46078800	-3.39048600
C	1.26252800	-1.46051200	3.39056100
C	-4.31513400	-1.44963400	-0.39367400
C	4.31525300	-1.44915800	0.39382100
C	-1.60383700	-1.03946900	3.41402800
C	1.60395900	-1.03942100	-3.41397400
C	-4.33128800	-1.04041100	1.00274500
C	4.33152000	-1.03999800	-1.00266400
C	-2.90928600	-0.82679900	2.84662100
C	2.90941900	-0.82657800	-2.84653600
C	-3.38913300	-0.49369600	-2.51166400
C	3.38904800	-0.49324300	2.51176100
C	-4.28916100	-0.38803000	-1.37531400
C	4.28903200	-0.38753800	1.37539400
C	-0.72172400	-0.12229900	-3.62813500
C	0.72167500	-0.12211000	3.62818500
C	-0.71735600	0.09834600	3.62992500
C	0.71733400	0.09831200	-3.62990500
C	-4.28686500	0.36202300	1.38160900
C	4.28697800	0.36243500	-1.38157600
C	-3.38617200	0.46827900	2.51830300
C	3.38622000	0.46857600	-2.51828900
C	-2.91261900	0.80160200	-2.84196800
C	2.91244800	0.80198900	2.84207000
C	-4.33460100	1.01449900	-0.99713500
C	4.33436300	1.01496300	0.99719600
C	-1.60787300	1.01526100	-3.41195600
C	1.60769600	1.01551000	3.41198700
C	-4.31714000	1.42442900	0.40079600
C	4.31700100	1.42486600	-0.40073300
C	-1.25816100	1.43638100	3.39428300
C	1.25801000	1.43644200	-3.39429700
C	-3.51227600	1.73843100	-1.93683200
C	3.51197300	1.73882400	1.93688800
C	-2.58191000	1.61836200	2.78984800
C	2.58178500	1.61858800	-2.78985800
C	-1.06384500	2.29770600	-3.24253800
C	1.06353500	2.29786500	3.24251700
C	-3.60646200	2.61045300	0.73122700
C	3.60619000	2.61082000	-0.73119600
C	-0.34447700	2.50945700	3.25261800
C	0.34418400	2.50946200	-3.25266400
C	-2.83398600	2.74266400	1.95601400
C	2.83371500	2.74295300	-1.95602700
C	-2.84393900	2.96374700	-1.61358100
C	2.84353500	2.96404300	1.61360200
C	-1.66649000	3.27235600	-2.33451000
C	1.66605900	3.27253300	2.33448900
C	-2.94108900	3.43591100	-0.27380800
C	2.94068000	3.43620900	0.27382100
C	-0.61389600	3.63176500	2.39108000
C	0.61347800	3.63183400	-2.39113200
C	-1.81649800	3.71942400	1.71809700
C	1.81609000	3.71962000	-1.71812100
C	-0.61340200	4.04125300	-1.75272900
C	0.61291300	4.04130700	1.75269600
C	-1.84950700	4.12937400	0.33144300
C	1.84904400	4.12958400	-0.33145600
C	-0.63451100	4.40362300	-0.37197500
C	0.63399600	4.40369000	0.37196400

Ce	-2.05739300	0.03114800	-0.00423800
Ce	2.05751500	0.03118800	0.00379300
O	0.00002800	0.37927400	0.00113700

(2) The coordinates of optimized $Ce_3N@D_2(35)$-C_{88}

C	-4.43472600	0.70088600	0.36370600
C	-4.51396600	-0.59962800	-0.36551900
C	-4.13425100	1.91459400	-0.35239500
C	-4.29837200	-1.85283800	0.36012900
C	-4.04871500	0.69187300	1.74267800
C	-4.09867700	-0.58382200	-1.74095700
C	-3.72821100	1.86406300	-1.71981400
C	-3.81450100	-1.77218900	1.72431700
C	-3.64646700	0.62707300	-2.37284500
C	-3.66445100	-0.53289400	2.38279200
C	-3.40924900	3.01563100	0.25406300
C	-3.59010600	-2.99798700	-0.25623500
C	-3.26293700	1.75610000	2.32853000
C	-3.32329800	-1.68010800	-2.32116500
C	-2.93335500	2.91998300	1.58659700
C	-3.06377500	-2.89122000	-1.60740100
C	-2.72997100	2.85476800	-1.96522400
C	-2.81912700	-2.77589800	1.95977100
C	-2.51625800	0.33288100	-3.19876800
C	-2.52997900	-0.26870700	3.22244100
C	-2.57907500	3.64600200	-0.74878200
C	-2.71472900	-3.57327300	0.75375800
C	-2.29844600	1.14538100	3.20837800
C	-2.32336400	-1.08316900	-3.18296400
C	-1.59854200	2.57626000	-2.78776500
C	-1.66576400	-2.52648800	2.80544200
C	-1.69746600	3.57975800	1.89946800
C	-1.80849700	-3.52021300	-1.90689000
C	-1.42506700	1.23685100	-3.36367500
C	-1.46229700	-1.19584000	3.38470400
C	-1.38104900	4.37270500	-0.43870300
C	-1.46967900	-4.23313500	0.43975500
C	-0.99441600	1.66652000	3.37804700
C	-1.03180800	-1.64238900	-3.37370300
C	-0.96805800	4.40616400	0.96065900
C	-1.06465500	-4.27693400	-0.93067400
C	-0.76339300	2.96718100	2.80147700
C	-0.84539600	-2.94548800	-2.82417800
C	-0.44616100	3.38191300	-2.54070100
C	-0.53370700	-3.34227000	2.57247000
C	-0.32627600	4.31922100	-1.42392300
C	-0.43371800	-4.20653600	1.41562300
C	-0.10016000	0.68481200	-3.60238500
C	-0.12260400	-0.67794700	3.63030400
C	0.12204900	0.77217500	3.60568700
C	0.10628200	-0.77229900	-3.59178600
C	0.44158100	4.35266700	1.34128600
C	0.32577800	-4.25355500	-1.29667900
C	0.53761100	3.43772500	2.48050500
C	0.44970300	-3.42037000	-2.47378100
C	0.84224600	2.87345300	-2.85315800
C	0.77278300	-2.89384000	2.91307900
C	1.08369800	4.34801700	-1.04575900
C	0.95598700	-4.27543600	1.04998400
C	1.03907200	1.55538100	-3.39763000
C	0.99232600	-1.58261800	3.43278500
C	1.49677000	4.34664800	0.35236200
C	1.36245500	-4.27868100	-0.31982200
C	1.46242200	1.28488500	3.35622300
C	1.43377100	-1.32069900	-3.33381500

C	1.79192100	3.48361900	-1.96540100
C	1.71620400	-3.51344600	2.00846700
C	1.66933700	2.60578700	2.74631300
C	1.60746400	-2.64520200	-2.73031000
C	2.32963700	1.00426800	-3.21433300
C	2.29448200	-1.05944800	3.22904600
C	2.67578400	3.59696600	0.67994700
C	2.62862900	-3.66754700	-0.65553100
C	2.52994400	0.35106000	3.21752400
C	2.52554300	-0.41586700	-3.19400200
C	2.80612400	2.83282800	1.91631000
C	2.76442800	-2.91256400	-1.88867700
C	3.00908900	2.80130200	-1.63574700
C	2.97520300	-2.91318700	1.68450800
C	3.30825800	1.60991200	-2.34970400
C	3.26670500	-1.69750100	2.36969500
C	3.48793900	2.91935600	-0.30666000
C	3.50432900	-3.07465600	0.34085600
C	3.66585600	0.59464900	2.38176500
C	3.65689700	-0.69029800	-2.35261600
C	3.77760500	1.80900000	1.69545000
C	3.78678400	-1.92594100	-1.67478700
C	4.06768100	0.54059400	-1.73950800
C	4.07352700	-0.64152600	1.76870300
C	4.18441000	1.81460500	0.32689400
C	4.25074900	-1.97377100	-0.30089300
C	4.45285200	0.57704400	-0.35972200
C	4.49063900	-0.70541800	0.39845700
Ce	0.02802100	2.17421300	0.00850800
Ce	-1.88907400	-1.08181400	-0.01694100
N	-0.00448000	-0.00391400	0.04086800
Ce	1.85043900	-1.12913900	-0.07573700

4. **References**

[S1] Hong, W.; Manrique, D. Z.; Moreno-García, P.; Gulcur, M.; Mishchenko, A.; Lambert, C. J.; Bryce, M. R.; Wandlowski, T. Single molecular conductance of tolanes: Experimental and theoretical study on the junction evolution dependent on the anchoring group. *J. Am. Chem. Soc.* **2011,** *134*, 2292-2304.